

Temperature and pressure dependences of the dielectric properties of PbF_2 and the alkaline-earth fluorides*

G. A. Samara

Sandia Laboratories, Albuquerque, New Mexico 87115

(Received 5 November 1975)

The effects of temperature and hydrostatic pressure on the real (ϵ') and imaginary (ϵ'') parts of the static dielectric constant of single crystals of PbF_2 , BaF_2 , SrF_2 , and CaF_2 were investigated. In all cases ϵ' decreases with increasing pressure. However, unlike the alkaline-earth fluorides and other normal ionic dielectrics where ϵ' increases slowly with increasing temperature, ϵ' of cubic PbF_2 exhibits a relatively large decrease with increasing temperature and obeys a Curie-Weiss law over a substantial temperature range. It is suggested that this anomalous temperature dependence and the large value of ϵ' (≈ 30) are associated with a soft long-wavelength transverse optic phonon, i.e., a ferroelectric (FE) mode, although the crystal remains stable with respect to this mode down to the lowest temperatures. This is the first example of a soft FE mode in a crystal having the relatively simple cubic fluorite structure. The measured isobaric temperature dependence of ϵ' is separated into its pure-volume and pure-temperature contributions. For the alkaline-earth fluorides both contributions are positive and additive, whereas for cubic PbF_2 the pure-temperature contribution is negative and dominates the measured $\epsilon'(T)$ response. This is attributed to the dominance of quartic anharmonicities in this crystal—a circumstance similar to that in other soft-FE-mode crystals. The Szigeti effective charges were calculated and the validity of the Lyddane-Sachs-Teller relationship was tested for all crystals. The effects of the pressure-induced cubic ($Fm\bar{3}m-O_h^5$) to orthorhombic ($Pmn2_1-V_{2h}^{16}$) phase transition on the dielectric properties of PbF_2 and BaF_2 were also investigated, and the possible lattice-dynamical origin of the transition is briefly discussed. In PbF_2 the orthorhombic phase is recovered at ambient conditions after releasing the pressure, and the effects of temperature and pressure on the dielectric properties of this phase were investigated. Unlike cubic PbF_2 , the orthorhombic phase behaves as a normal ionic dielectric. At $T \geq 300^\circ\text{K}$ the dielectric loss in both phases of PbF_2 becomes very large due to the high ionic conductivity of the material. The activation energies deduced from the loss data are in excellent agreement with those obtained from ionic conductivity measurements.

I. INTRODUCTION

This paper deals with the effects of temperature and hydrostatic pressure on the dielectric properties of PbF_2 and the alkaline-earth fluorides CaF_2 , SrF_2 , and BaF_2 . These crystals, which crystallize in the cubic fluorite structure, constitute an important class of relatively simple ionic crystals whose optical and lattice-dynamical properties are of much theoretical and experimental interest. The dielectric constants play an important role in these as well as most other properties of these crystals. It is therefore necessary to understand the dielectric constants and their temperature and volume dependences in terms of the various mechanisms of dielectric polarization. Toward this end the combination of temperature and pressure measurements makes it possible to separate the isobaric temperature dependences of the dielectric constants into their explicit volume and temperature contributions. The explicit temperature contributions arise from anharmonic effects, and, as we shall see, they play an especially significant role in determining the interesting properties of PbF_2 .

Apparently there are no previous measurements of the static dielectric constant of PbF_2 . The pres-

ent results show that, unlike normal ionic dielectrics, including the alkaline-earth fluorides, the dielectric constant of PbF_2 increases with decreasing temperature and obeys a Curie-Weiss law. It is suggested that this behavior and the large value of the dielectric constant are associated with the existence in PbF_2 of a soft long-wavelength transverse optic phonon, i.e., a ferroelectric mode.

We measured the temperature and pressure dependences of the static dielectric constants of the alkaline-earth fluorides several years ago. The results were not published since several papers have since appeared on the subject.¹⁻³ However, since there are substantial quantitative differences among the results of the various authors, we shall give a brief account of our results here. An additional and more important reason for presenting our results is that it is instructive to compare, for possible systematic trends, the results on PbF_2 and those on the alkaline-earth fluorides. Such comparisons are made more meaningful by minimizing systematic experimental uncertainties—hence the desirability to compare results obtained using the same experimental techniques.

It is known that the present crystals undergo pressure-induced phase transitions from the fluo-

rite to an orthorhombic phase. We have studied the effects of this transition on the dielectric properties of PbF_2 and BaF_2 . There appears to be no such previous studies except for a brief account on BaF_2 by the present author.⁴ In the case of PbF_2 , the orthorhombic phase is recovered at ambient conditions after releasing the pressure, which allows one to investigate the temperature dependence of the dielectric constant of this phase over a wide range. Such results will be reported here.

The paper is organized as follows: Sec. II describes the experimental details and Sec. III presents the results. These results and their interpretation in terms of macroscopic and microscopic models are discussed in Sec. IV, and followed by a brief overall summary and conclusions in Sec. V.

II. EXPERIMENTAL DETAILS

Single crystals of cubic PbF_2 , BaF_2 , SrF_2 , and CaF_2 were purchased from Harshaw. Samples were cut in the form of thin plates 0.5–1.0-mm thick and 0.6–1.0 cm^2 in area and were generally oriented with the thickness dimension along one of the cubic axes. Chrome-gold or aluminum electrodes were vapor deposited on the large sample faces. Capacitance and dielectric loss measurements were made in the frequency range 1 kHz–1 MHz employing transformer ratio arm bridges (General Radio Model 1615A or Hewlett-Packard Model 4270A) equipped with three terminal connections. Shielded leads and sample holders were used.

Pressure measurements at and above room temperature were performed in a 30-kbar (=3.0 GPa) apparatus using a 50:50 mixture of normal- and iso-pentane as pressure fluid. The general experimental procedures have been given elsewhere.⁵

Measurements below room temperature were performed in beryllium copper or maraging steel cells mounted inside conventional low-temperature Dewars. Helium gas was the pressure fluid, and the pressure was measured to better than 1% by either a Heise Bourdon tube gauge or a calibrated manganin gauge. Temperature changes were measured to $\pm 0.10^\circ\text{K}$ using Cu-constantan and Cu-AuFe thermocouples.

The real (ϵ') and imaginary (ϵ'') parts of the dielectric constant and their changes with temperature and pressure were calculated from the measured sample capacitance and loss by correcting for changes in sample dimensions due to thermal expansion and compression.⁶ Values of the volume compressibilities κ , evaluated from available elastic constants c_{ij} , and thermal expansivities β are

given in Table I. For BaF_2 , SrF_2 , and CaF_2 the c_{ij} 's at different temperatures have been reported by Gerlich⁷ and Wong and Schuele.⁸ These c_{ij} 's yield the initial, or low pressure, κ . At the relatively high pressures reached in the present work, it is necessary to account for the pressure dependence of κ . To do so Bridgman's⁹ P - V data were also used. It should also be pointed out that the c_{ij} 's yield the adiabatic compressibility, whereas the isothermal compressibility is needed. However, the small difference between the two values is of no consequence for the present purposes.

For cubic PbF_2 the c_{ij} 's at room temperature were measured by Hart.¹⁰ The values of κ at other temperatures (in Table I) for this crystal are estimates based on the assumption that the temperature dependence of κ is similar to that of BaF_2 , SrF_2 , and CaF_2 . The volume change at the transition in PbF_2 can be deduced from the lattice parameters given by Schmidt and Vedam.¹¹

Values of β for BaF_2 , SrF_2 , and CaF_2 for temperatures between 4 and 300°K have been reported by Bailey and Yates.¹² For cubic PbF_2 , β was determined between 75 and 300°K from x-ray lattice parameter data obtained by Morosin.¹³

Apparently neither κ nor β have been measured for orthorhombic PbF_2 . Therefore we used the values of the cubic phase in the present analysis. One can readily show that uncertainties introduced by the above approximations do not affect the main conclusions of the paper.

III. RESULTS

A. Alkaline-earth fluorides

As mentioned earlier, the effects of pressure and temperature on the static dielectric constants of BaF_2 , SrF_2 , and CaF_2 have been reported by others. Since our results on these crystals are generally in agreement with some of the published results, a brief account of the present results suffices.

Figure 1 shows the temperature dependence of ϵ' of BaF_2 at 1 bar. The results are independent of frequency in the 1–1000 kHz range and the dielectric loss for the crystal used is very low, with $\tan\delta < 0.007$ at room temperature. It is seen that ϵ' decreases smoothly with decreasing T and approaches 0°K with zero slope $(\partial\epsilon'/\partial T)_P$, as it must. This is the usual behavior for normal ionic crystals. The data for SrF_2 and CaF_2 are qualitatively similar and in close agreement with those of Lowndes,² and hence are not shown. The logarithmic temperature derivatives for all three crystals are given in Table I and compared with results from other authors.

Figure 2 shows the pressure dependence of ϵ' at

TABLE I. Values of the volume thermal expansion (β) and compressibility (κ) and the logarithmic pressure and temperature derivatives of the capacitance (C) and dielectric constant (ϵ').

Crystal	T (°K)	β ($10^{-5}/^{\circ}\text{K}$)	κ ($10^{-3}/\text{kbar}$)	$(\partial \ln C / \partial P)_T$ ($10^{-3}/\text{kbar}$)	$(\partial \ln \epsilon' / \partial P)_T$ ($10^{-3}/\text{kbar}$)	$(\partial \ln C / \partial T)_P$ ($10^{-5}/^{\circ}\text{K}$)	$(\partial \ln \epsilon' / \partial T)_P$ ($10^{-5}/^{\circ}\text{K}$)
PbF ₂ (cubic)	16.3	~0	1.53	-10.75 ± 0.35	-10.24	- 8.7 ± 0.8	- 8.7
	75.6	7.52	1.54	-10.22 ± 0.30	- 9.71	-36.0 ± 0.6	-38.5
	180.0	7.51	1.59	- 9.60 ± 0.30	- 9.07	-27.0 ± 0.6	-29.5
	295.0	7.50	1.65	- 8.60 ± 0.30	- 8.05	-21.5 ± 0.8	-24.0
PbF ₂ (ortho.)	75.6	7.52	1.54	- 4.34 ± 0.25 ^a	- 3.83	43.0 ± 1.5	40.5
	290.0	7.50	1.65	- 6.30 ± 0.30	- 5.75	51.5 ± 2.0	49.0
BaF ₂	20.0	0.03	1.60	- 3.60 ± 0.10	- 3.07	0.7 ± 0.2	0.6
	75.6	2.10	1.61	- 4.20 ± 0.10	- 3.67	15.9 ± 0.4	15.2
	295.0	5.60	1.77	- 4.78 ± 0.15	- 4.18	23.5 ± 0.5	21.6
	308.0			- 4.99 ^b		23.1 ^b	
	300.0			- 5.89 ^c		24.4 ^c	
	298.0			- 4.85 ^d		...	
SrF ₂	295.0	5.45	1.43	- 4.00 ± 0.15	- 3.52	22.7 ± 0.5	20.9
	308.0			- 4.04 ^b		22.8 ^b	
	300.0			- 5.28 ^c		24.7 ^b	
CaF ₂	295.0	5.70	1.22	- 3.65 ± 0.15	- 3.24	26.6 ± 0.5	24.7
	308.0			- 3.78 ^b		26.3 ^b	
	300.0			- 4.37 ^c		24.8 ^c	
	296.0			- 4.59 ^d		...	
	291.0			- 3.81 ^d		...	

^a Slope at $P > 1.0$ kbar. See Fig. 9.^b Data from Ref. 3.^c Data from Ref. 2.^d Data from Ref. 1.

295 °K for the three crystals expressed as fractional changes in simple capacitance. The data extend to much higher pressure than has been reported, and it is seen that $\epsilon'(P)$ for each crystal is nonlinear over the pressure range covered. For BaF₂ measurements were also made at 75.6 and 20.0 °K but over a lower pressure range. The initial (i.e., $P = 0$) logarithmic pressure derivatives are given in Table I and compared with those of others. The present values are in close agreement with those of Jones¹ and Andeen *et al.*³

The 295-°K results on BaF₂ were extended through the cubic-orthorhombic transition pressure⁴ and are shown in Fig. 3. This transition is strongly first order ($\Delta V \approx 11\%$) with a large hysteresis and has been discussed earlier.⁴ As shown below, PbF₂ exhibits a similar pressure-induced transition.

B. Lead fluoride

1. Cubic phase

The temperature dependence of ϵ' at 1 bar is shown in Fig. 1. Below ~230 °K there is no frequency dependence of ϵ' between 1 and 1000 kHz, but strong frequency dependence is observed at

higher temperatures. In this high-temperature regime the dielectric loss $\tan \delta$ is also frequency dependent and increases very rapidly with T . This is shown in Fig. 4, expressed as $\epsilon'' (= \epsilon' \tan \delta)$. It is seen that ϵ'' increases exponentially with T . As will be discussed later, this increase in ϵ' and ϵ'' is attributed to dipolar contributions associated with the activation and formation of lattice defects.

In Fig. 1 the 1-MHz curve represents the true $\epsilon'(T)$ response of cubic PbF₂ up to ~320 °K. Unlike the behavior of normal ionic crystals such as BaF₂, ϵ' of cubic PbF₂ increases with decreasing T and the magnitude of ϵ' is much larger than for the other fluorides studied. The explanation of these features is given in Sec. IV.

Figure 5 shows the pressure dependence of ϵ' at different temperatures measured either at 100 or 1000 kHz where ϵ' is independent of frequency. The $\epsilon'(P)$ responses are essentially linear over the limited pressure range covered. The dielectric loss also decreases with pressure.

Table I gives a summary of the logarithmic temperature and pressure derivatives. Apparently there are no previous measurements to compare with.

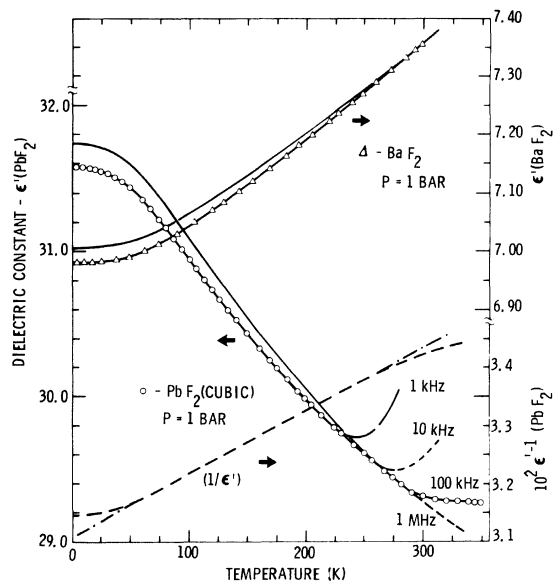


FIG. 1. Temperature dependence of the real part of the static dielectric constant for cubic PbF_2 and BaF_2 . Symbols represent the measured responses whereas the solid lines represent the results corrected for the thermal expansion of the samples. Also shown is the temperature dependence of the inverse dielectric constant for PbF_2 . Note that this response is linear between ~ 50 and ~ 270 °K.

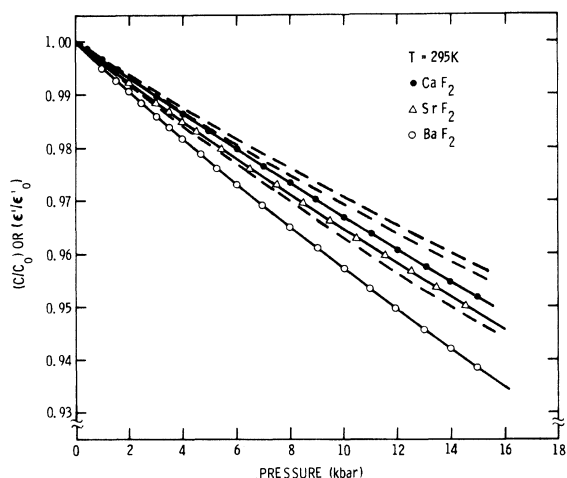


FIG. 2. Pressure dependence of the real part of the static dielectric constant for cubic BaF_2 , SrF_2 , and CaF_2 . Symbols represent the measured response whereas the dashed lines represent the results corrected for the compression of the samples.

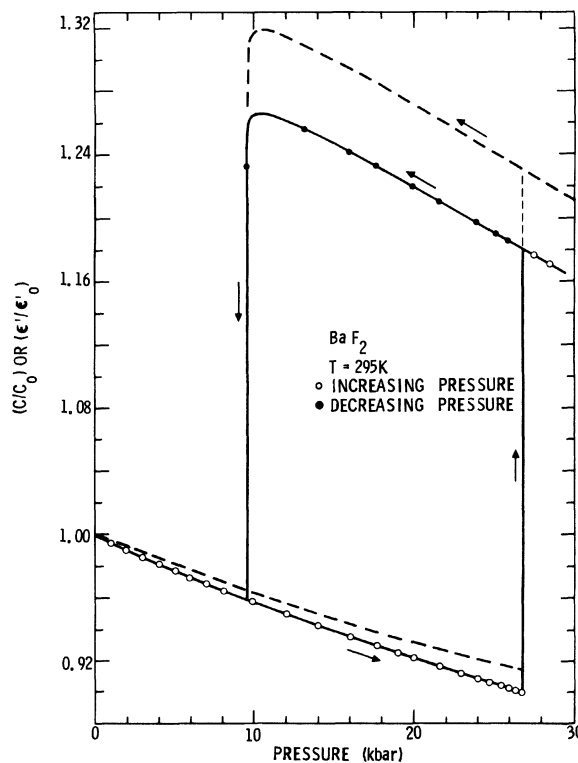


FIG. 3. Pressure dependence of the real part of the static dielectric constant of BaF_2 showing the behavior across the cubic-orthorhombic phase transition. Symbols represent the measured response whereas the dashed lines represent the results corrected for the compression of the sample.

2. Cubic \rightarrow orthorhombic transition

Figures 6 and 7 show the variations of ϵ' and ϵ'' with pressure across the cubic \rightarrow orthorhombic phase transition at various frequencies. The transition is first order. At 1 kHz the crystal is very lossy in both phases, and the $\epsilon'(P)$ response in Fig. 6 is strongly influenced by the high loss of the crystal. Also, since the transition is reconstructive and accompanied by a large decrease in volume ($\Delta V/V_0 \approx -10\%$), a very large number of crystalline defects result. In fact, the clear, transparent crystals become milky white after going through the transition. Some of the defects are apparently polar and mobile at low frequencies in the orthorhombic phase resulting in high values of ϵ' . The large decrease in ϵ' with pressure at 1 kHz in the orthorhombic phase is most likely associated with some annealing of defects. In this region, and especially just above the transition, ϵ' decreases with time at constant P . At 1 MHz many of the polar defects

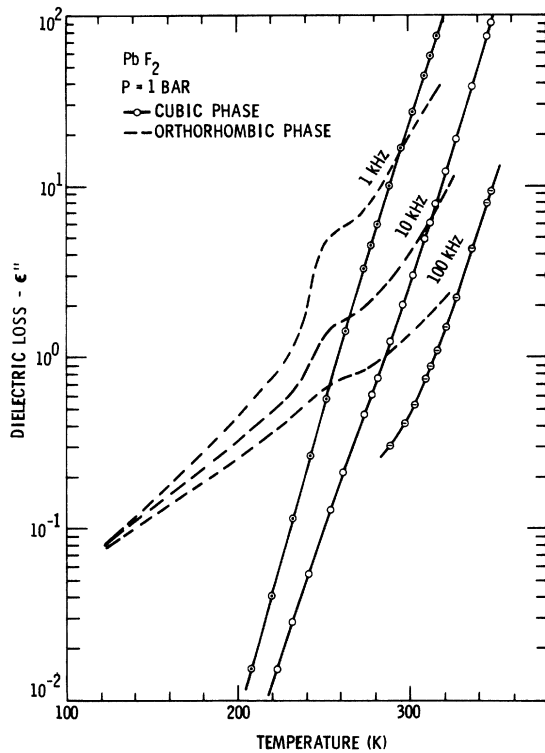


FIG. 4. Temperature dependence of the imaginary part of the dielectric constant measured at different frequencies for both cubic and orthorhombic PbF_2 .

apparently become immobile, the dielectric loss becomes much smaller, and the $\epsilon'(P)$ response approaches the true response of the material.

The transition exhibits strong kinetics effects. At room temperature it initiated at pressures between 3.93 and 4.75 kbar, depending on how long the pressure is held constant in the vicinity of the transition. The 3.93-kbar point was determined by increasing the pressure to this value and holding it constant. The transition started after about 20 min. The higher transition pressure values were determined in the usual manner of making the present measurements, namely, raising the pressure in steps (usually 0.1–0.3 kbar), waiting 5–10 min at each step for the temperature of the pressure fluid (pentane) to return to equilibrium, and then taking the readings. These observations emphasize that the cubic phase exists metastably over a wide pressure range.

3. Orthorhombic phase

As indicated in Figs. 6 and 7, the cubic \rightarrow orthorhombic transition is not reversible, and the orthorhombic phase is recovered upon release of the pressure. Recovered samples are stable and their dielectric properties exhibit reversible and

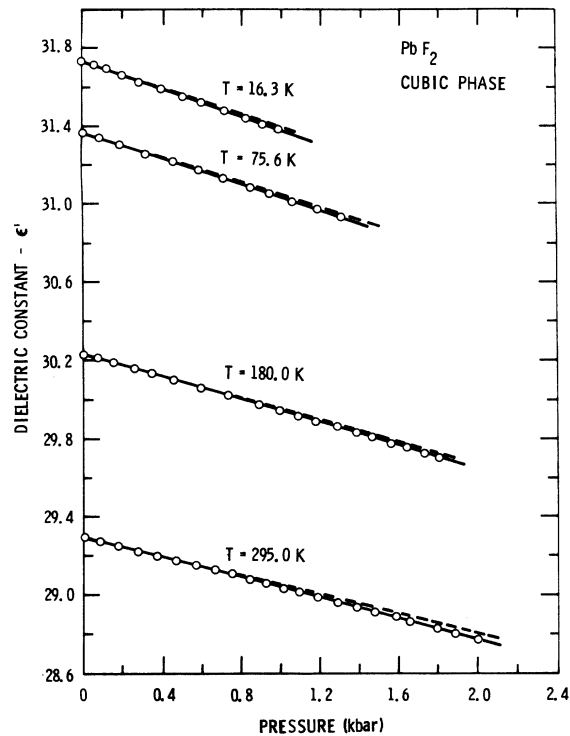


FIG. 5. Pressure dependence of the real part of the static dielectric constant at different temperature for cubic PbF_2 . Symbols represent the measured response whereas the dashed lines represent the results corrected for the compression of the sample.

reproducible temperature and pressure changes.

The temperature dependences of ϵ'' and ϵ' of orthorhombic PbF_2 at 1 bar are shown in Figs. 4 and 8, respectively. Below 300°K, ϵ'' is considerably larger than in the cubic phase (undoubtedly owing to the large number of defects in the recovered orthorhombic samples), and this contributes to the much larger frequency dependence of ϵ' in Fig. 8. In Fig. 8 the $\epsilon'(T)$ response becomes frequency independent above ~ 500 kHz, and the 1-MHz curve should represent the true response of the material.

In Fig. 8 a shoulder centered about 250°K appears in the $\epsilon'(T)$ response at 1 and 10 kHz. The origin of this feature is not known, but it may be associated with a dipolar impurity or defect. The $\epsilon''(T)$ data in Fig. 4 show that the shoulder is more pronounced here and persists to over 100 kHz.

Comparing Figs. 8 and 1 shows that, unlike cubic PbF_2 , the orthorhombic phase exhibits a normal $\epsilon'(T)$ response, i.e., ϵ' decreases with decreasing temperature. The magnitude of ϵ' is, however, still high.

Figure 9 shows the pressure dependence of ϵ' .

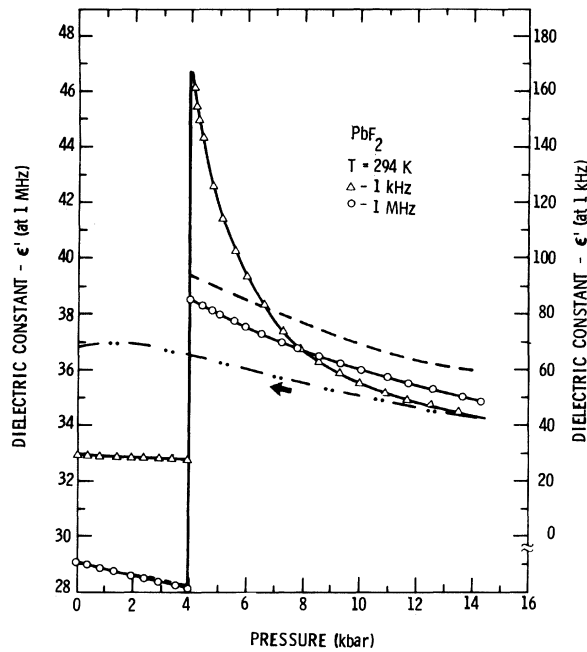


FIG. 6. Pressure dependence of the real part of the static dielectric constant of PbF_2 showing the behavior across the cubic-to-orthorhombic phase transition. At 1 kHz the crystal is very lossy and the 1-MHz data are more representative of the real response of the crystal. Symbols represent the measured responses whereas the dashed lines (shown for the 1-MHz data only) represent the results corrected for the compression of the sample. Note that the transition is not reversible as evidenced by the response on lowering the pressure (shown by the dot-dash curve at 1 kHz).

At 290 °K, ϵ' decreases with pressure as is the case for normal ionic crystals. However, at 75.6 °K, ϵ' first increases, goes through a broad maximum at ~ 0.5 kbar, and then decreases. The effects are reversible. The cause of the initial increase and maximum is not understood.

The logarithmic temperature and pressure derivatives of ϵ' for orthorhombic PbF_2 are summarized and compared with those of the other crystals in Table I.

IV. DISCUSSION

We now wish to examine the implications of the results presented in Sec. III with special emphasis given to PbF_2 . We first examine the results from a macroscopic point of view and then proceed to the microscopic aspects.

A. Macroscopic treatment

The isobaric temperature dependence of ϵ' for cubic or isotropic substances derives from two

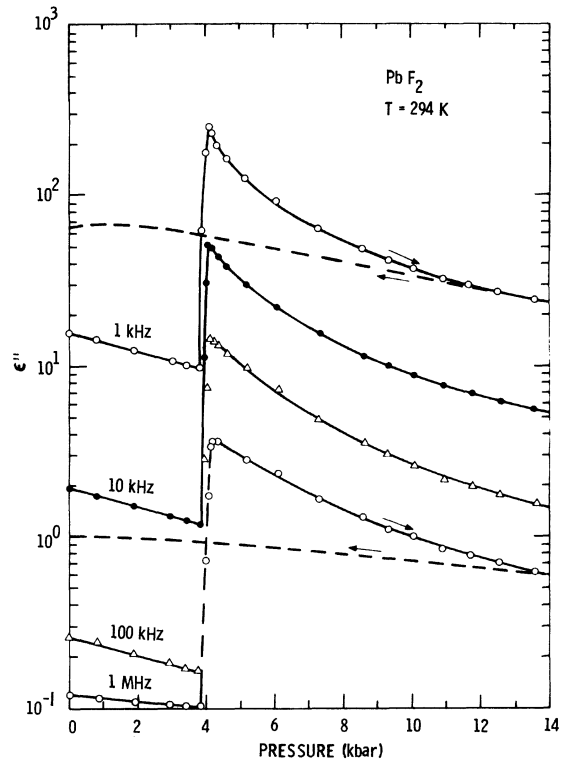


FIG. 7. Pressure dependence of the imaginary part of the dielectric constant of PbF_2 at different frequencies showing the behavior across the cubic-to-orthorhombic transition. Note that the transition is irreversible.

contributions: (i) the contribution associated with the change in volume V , i.e., the explicit-(pure-) volume effect, and (ii) the explicit-(pure-) temperature dependence which would occur even if the volume of the sample were held constant. Writing $\epsilon' = \epsilon'(V, T)$ we can evaluate the two contributions to the measured $\epsilon'(T)$ over the whole range of the measurements. To do so we write

$$(\Delta\epsilon'_T)_P = -(\Delta\epsilon'_P)_T + (\Delta\epsilon'_T)_V, \quad (1)$$

where in this notation $(\Delta\epsilon'_T)_P$ is the measured change in ϵ' on raising the temperature from 0 to T °K at 1 bar; $(\Delta\epsilon'_T)_V$ is the change in ϵ' caused by raising the temperature from 0 to T °K at constant volume, that being the volume of the sample at 0 °K and 1 bar; $-(\Delta\epsilon'_P)_T$ is the change in ϵ' caused by raising the pressure at constant temperature T from 1 bar to a value P sufficient to produce a volume change equal in magnitude to that caused by raising the temperature from 0 to T °K at 1 bar. This last term is readily evaluated from $\epsilon'(P)$ data and the known β and κ , and it obviously enters with a negative sign since the signs of β and κ are normal for the crystals of interest here, i.e., ΔV is positive on heating and

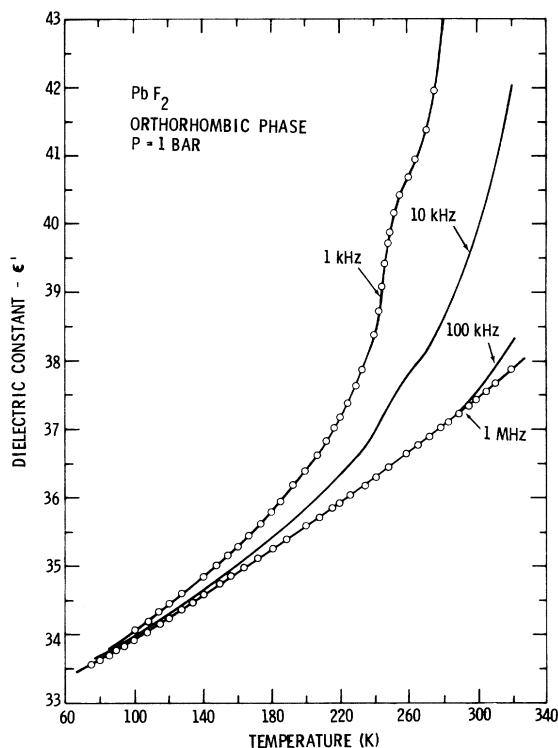


FIG. 8. Temperature dependence of the real part of the static dielectric constant for orthorhombic PbF_2 at different frequencies. Dielectric loss is large at low frequencies, and the 1-MHz curve is more representative of the response of the orthorhombic phase. Data have not been corrected for the thermal expansion of the sample. Corrections would be quite small on the scale of this figure (cf. Fig. 1).

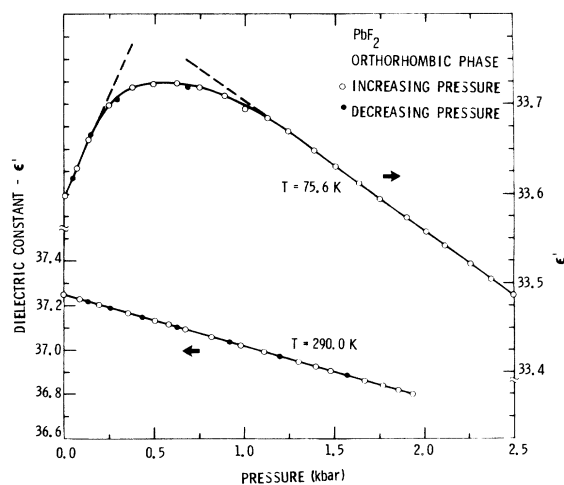


FIG. 9. Pressure dependence of the real part of the static dielectric constant of orthorhombic PbF_2 at different temperatures measured at 1 MHz. Data have not been corrected for the compression of the sample. Corrections are small (cf. Fig. 5).

negative on compression. Figure 10 shows the results of the analysis for cubic PbF_2 and BaF_2 . The results clearly show the marked contrast between PbF_2 and BaF_2 which qualitatively typifies the other alkaline-earth fluorides and other normal dielectrics. For BaF_2 both the pure-volume effect $-(\Delta\epsilon'_p)_T$ and the pure-temperature effect $(\Delta\epsilon'_T)_V$ are positive and add to yield the measured isobaric change in ϵ' . For cubic PbF_2 , on the other hand, the two effects are of opposite sign and act to cancel each other, but the pure-temperature effect dominates the observed isobaric decrease of ϵ' with increasing T .

The results can be examined from a more fundamental viewpoint. The dielectric constant is determined by the electrical polarizability of the medium, and for a cubic or isotropic crystal the macroscopic Clausius-Mossotti relationship

$$(\epsilon' - 1)/(\epsilon' + 2) = (\frac{4}{3}\pi)(\alpha/V) \quad (2)$$

holds.^{14,15} Here α is the total polarizability of a macroscopic small sphere of volume V . The logarithmic temperature and pressure derivatives of Eq. (2) at constant pressure are:

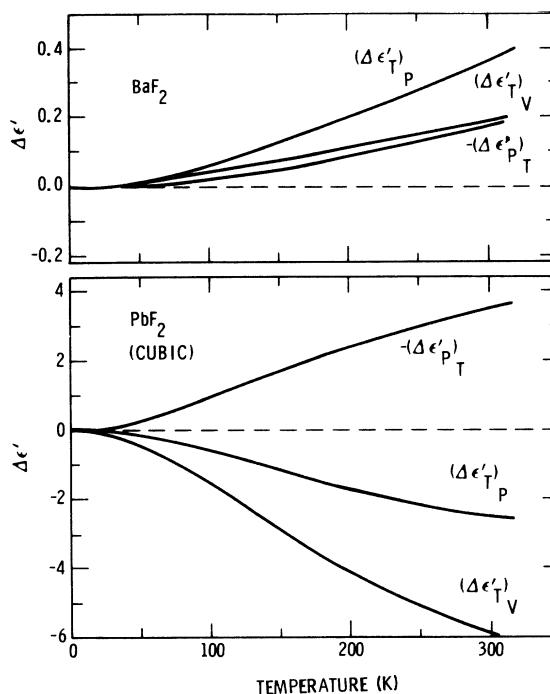


FIG. 10. Separation of the measured change in the real part of the static dielectric constant with temperature $(\Delta\epsilon'_p)_T$ into its pure-volume $-(\Delta\epsilon'_p)_T$ and pure-temperature $(\Delta\epsilon'_T)_V$ contributions for cubic PbF_2 and BaF_2 .

$$\frac{3\epsilon'}{(\epsilon'-1)(\epsilon'+2)} \left(\frac{\partial \ln \epsilon'}{\partial T} \right)_P = -\beta + \beta \left(\frac{\partial \ln \alpha}{\partial \ln V} \right)_T + \left(\frac{\partial \ln \alpha}{\partial T} \right)_V, \quad (3)$$

$$\frac{3\epsilon'}{(\epsilon'-1)(\epsilon'+2)} \left(\frac{\partial \ln \epsilon'}{\partial P} \right)_T = \kappa - \kappa \left(\frac{\partial \ln \alpha}{\partial \ln V} \right)_T. \quad (4)$$

The left-hand sides simply represent the fractional changes in the quantity $(\epsilon' - 1)/(\epsilon' + 2)$ and the interpretations of the various contributions to Eqs. (3) and (4) have been presented earlier.^{6,14}

All quantities in Eqs. (3) and (4) are known or can be evaluated except $(\partial \ln \alpha / \partial T)_V$, which is then determined by substitution.

Values for each quantity are given in Table II for the crystals of interest. The fact that ϵ' decreases with pressure clearly shows that the change in polarizability with volume, i.e., the contribution $-\kappa(\partial \ln \alpha / \partial \ln V)_T$, dominates the pressure dependence of ϵ' , since the change in density, i.e., the contribution κ , would make ϵ increase with pressure. The results in Table II make this conclusion quantitative. We also note that $(\partial \ln \alpha / \partial \ln V)_T$ is $\sim 1-2$ for all of these crystals as has been found to be the case for many other ionic crystals.^{6,14,16}

For the temperature dependence of ϵ' , the two volume-dependent contributions, $-\beta$ and $\beta(\partial \ln \alpha / \partial \ln V)_T$ have opposite signs, but their sum, i.e., the total volume-dependent effect, is positive for all the crystals; again emphasizing the dominance of the change of α with volume. The pure-temperature contribution $(\partial \ln \alpha / \partial T)_V$ is also positive (except for cubic PbF_2), and it enhances the total

volume effect in causing ϵ to increase with T . For cubic PbF_2 , on the other hand, $(\partial \ln \alpha / \partial T)_V$ is negative and is responsible for the observed anomalous decrease of ϵ' with increasing T .

The total macroscopic polarizability α arises from two different contributions—an electronic contribution α_{el} and an ionic (infrared) contribution α_{ir} —and we can write^{6,14}

$$\alpha = \alpha_{\text{el}} + \alpha_{\text{ir}}. \quad (5)$$

α_{el} is related to the high-frequency dielectric constant ϵ_∞ ($\equiv n^2$, where n is the refractive index in the limit of long wavelengths) by the Lorentz-Lorentz equation

$$\frac{\epsilon_\infty - 1}{\epsilon_\infty + 2} = \frac{n^2 - 1}{n^2 + 2} = \frac{4\pi}{3} \left(\frac{\alpha_{\text{el}}}{V} \right), \quad (6)$$

which is applicable to cubic crystals. This is of the same form as Eq. (2). From Eq. (5) it follows that

$$\left(\frac{\partial \ln \alpha}{\partial \ln V} \right)_T = \frac{\alpha_{\text{el}}}{\alpha} \left(\frac{\partial \ln \alpha_{\text{el}}}{\partial \ln V} \right)_T + \frac{\alpha_{\text{ir}}}{\alpha} \left(\frac{\partial \ln \alpha_{\text{ir}}}{\partial \ln V} \right)_T, \quad (7)$$

$$\left(\frac{\partial \ln \alpha}{\partial T} \right)_V = \frac{\alpha_{\text{el}}}{\alpha} \left(\frac{\partial \ln \alpha_{\text{el}}}{\partial T} \right)_V + \frac{\alpha_{\text{ir}}}{\alpha} \left(\frac{\partial \ln \alpha_{\text{ir}}}{\partial T} \right)_V. \quad (8)$$

To evaluate the various contributions in Eqs. (7) and (8), the temperature and pressure dependences of n are needed. The pressure dependence of n has been reported for CaF_2 , BaF_2 , and cubic PbF_2 by Schmidt and Vedam,¹¹ and the temperature dependence of n is known for CaF_2 ,¹⁷ and cubic PbF_2 .¹⁸ The results, summarized in Table III, allow us to assess the relative importance of the electronic and ir terms in Eqs. (7) and (8) for this

TABLE II. Various contributions to the pressure and temperature dependences of the static dielectric constant according to Eqs. (3) and (4).

Crystal	T (°K)	ϵ'	$K^* \left(\frac{\partial \ln \epsilon'}{\partial P} \right)_T^a$ ($10^{-4}/\text{kbar}$)	$= -\kappa \left(\frac{\partial \ln \alpha}{\partial \ln V} \right)_T + \kappa$ ($10^{-4}/\text{kbar}$)	$\left(\frac{\partial \ln \alpha}{\partial \ln V} \right)_T$	$K^* \left(\frac{\partial \ln \epsilon'}{\partial T} \right)_P^a$ ($10^{-5}/^\circ\text{K}$)	$= -\beta + \beta \left(\frac{\partial \ln \alpha}{\partial \ln V} \right)_T + \left(\frac{\partial \ln \alpha}{\partial T} \right)_V$ ($10^{-5}/^\circ\text{K}$)				
PbF_2 (cubic)	4.0	31.73	-9.4	= -24.7	+ 15.3	1.62	~ 0	= 0	0	0	0
	16.3	31.72	-9.4	= -24.7	+ 15.3	1.62	-0.83	= ~ 0	+ ~ 0	- 0.83	
	75.6	31.36	-9.0	= -24.4	+ 15.4	1.58	-3.58	= -7.52	+ 11.90	- 7.96	
	180.0	30.24	-8.7	= -24.6	+ 15.9	1.55	-2.84	= -7.51	+ 11.62	- 6.95	
	295.0	29.30	-8.0	= -24.5	+ 16.5	1.48	-2.38	= -7.50	+ 11.12	- 6.00	
PbF_2^b (ortho.)	75.6	33.6	-3.3	= -18.7	+ 15.4	1.22	3.50	= -7.52	+ 9.17	+ 1.85	
	290.0	37.3	-4.5	= -21.0	+ 16.5	1.28	3.85	= -7.50	+ 9.60	+ 1.75	
BaF_2	20.0	7.00	-12.0	= -28.0	+ 16.0	1.75	0.23	= -0.03	+ 0.05	+ 0.21	
	75.6	7.03	-14.2	= -30.3	+ 16.1	1.89	5.90	= -2.10	+ 3.96	+ 4.04	
	295.0	7.34	-15.5	= -33.2	+ 17.7	1.88	8.03	= -5.60	+ 10.50	+ 3.13	
SrF_2	295.0	6.48	-14.7	= -29.0	+ 14.3	2.03	8.76	= -5.45	+ 11.05	+ 3.16	
CaF_2	295.0	6.81	-12.9	= -25.1	+ 12.2	2.06	9.86	= -5.70	+ 11.73	+ 3.83	

^a $K^* = 3\epsilon' / (\epsilon' - 1)(\epsilon' + 2)$.

^b Values of β and κ assumed to be the same as for the cubic phase.

TABLE III. Values at 295 °K of the refractive index (n) and high-frequency dielectric constant (ϵ_∞) and its logarithmic pressure and temperature derivatives.

Crystal	n	ϵ_∞	$(\partial \ln \epsilon_\infty / \partial P)_T$ ($10^{-4}/\text{kbar}$)	$(\partial \ln \epsilon_\infty / \partial T)_P$ ($10^{-5}/^\circ\text{K}$)
PbF ₂	1.754	3.076	8.78 ^a	-2.83 ^b
CaF ₂	1.434	2.056	3.40 ^a	-0.84 ^c
BaF ₂	1.472	2.167	8.70 ^a	...

^a Values calculated from data in Ref. 11.

^b Values calculated from data in Ref. 18.

^c Values calculated from data in Ref. 17.

class of materials.

The quantities $(\partial \ln \alpha_{\text{el}} / \partial \ln V)_T$ and $(\partial \ln \alpha_{\text{el}} / \partial T)_V$ are determined from Eqs. (3) and (4) with ϵ' and α replaced by ϵ_∞ and α_{el} , respectively. The various contributions in Eqs. (7) and (8) are then readily determined and are given in Table IV. It is clear from the results that the quantities $(\partial \ln \alpha / \partial \ln V)_T$ and $(\partial \ln \alpha / \partial T)_V$ are predominantly determined by changes in α_{ir} . By comparison, effects due to changes in α_{el} are negligible to a first approximation. This conclusion seems to be characteristic of most ionic crystals.^{6,14,16}

The volume contribution to $\epsilon'(T)$ [$\beta(\partial \ln \alpha / \partial \ln V)_T$], which as seen above is largely due to the infrared term, is positive and dominates the pure-volume effect in all cases. It is in absolute magnitude generally the largest contribution to the T dependence of ϵ' (Table II). The positive sign of $(\partial \ln \alpha_{\text{ir}} / \partial \ln V)_T$ can be understood on simple arguments. For a classical ionic model, α_{ir} is inversely proportional to the restoring force between ions.^{6,14} As the lattice expands, the restoring force decreases and, therefore, α_{ir} increases so that $(\partial \ln \alpha_{\text{ir}} / \partial \ln V)_T$ is positive. This is the reason why ϵ' decreases with increasing pressure for all the crystals of the present interest (see Tables II and IV).

As can be seen from Table II, the pure-temperature effect $(\partial \ln \alpha / \partial T)_V$ is positive for all the crystals except cubic PbF₂. This effect, which according to Table IV is strongly dominated by $(\partial \ln \alpha_{\text{ir}} / \partial T)_V$, arises from anharmonic lattice ef-

fects. For a harmonic lattice, the restoring force constant is independent of amplitude and α_{ir} is thus independent of temperature, so that $(\partial \ln \alpha_{\text{ir}} / \partial T)_V = 0$. Anharmonicities on the other hand, cause the restoring force and hence α_{ir} to be amplitude or temperature dependent. For the treatment of such anharmonicities we must resort to the theory of anharmonic lattice dynamics.

B. Lattice-dynamical treatment

1. Harmonic model result

Results of harmonic lattice-dynamical treatments, such as the modified rigid-ion and shell models, allow us to express the static dielectric constant of a cubic ionic crystal of the MF₂ type as^{19,20}

$$\epsilon' = \epsilon_\infty + \frac{4\pi(Z_1 Z_2 e^{*2})}{v \omega_0^2} \left(\frac{1}{m_1} + \frac{1}{2m_2} \right) \left(\frac{\epsilon_\infty + 2}{3} \right)^2, \quad (9a)$$

$$= \epsilon_\infty + \eta_0, \quad (9b)$$

where ϵ_∞ is the high-frequency dielectric constant, v is the volume per molecule, ω_0 is the strictly harmonic long-wavelength ($\vec{q}=0$) transverse-optic (TO) mode frequency, i.e., the ir resonance frequency,²¹ $Z_{1,2}$ and $m_{1,2}$ are the ionic valences and masses of the metal and fluorine ions, respectively, and e^* is an effective ionic charge. In Eq. (9) ϵ_∞ is determined solely by the electronic polarizabilities of the ions, whereas the second contribution designated by η_0 represents the lattice contribution which is associated with the polar (transverse) displacements of the positive and negative ions.

Since real crystals are never strictly harmonic, Eq. (9) has to be applied with caution. At very low temperatures the only anharmonicities contributing to the measured values of ϵ' and ω_{TO} are those associated with zero-point motion, and for most ionic crystals these are quite small.²² Thus, to a good approximation, the measured values of ϵ' and ω_{TO} can be taken to represent the strictly harmonic values, and Eq. (9) can be used directly (e.g., to calculate e^* , as discussed later).

At high temperatures lattice anharmonicities

TABLE IV. Separation of the total polarizability α and its logarithmic volume and temperature derivatives into their electronic and lattice (ir) contributions at 295 °K.

Crystal	$\frac{\alpha_{\text{el}}}{\alpha}$	$\frac{\alpha_{\text{ir}}}{\alpha}$	$\left(\frac{\partial \ln \alpha}{\partial \ln V} \right)_T = \frac{\alpha_{\text{el}}}{\alpha} \left(\frac{\partial \ln \alpha_{\text{el}}}{\partial \ln V} \right)_T + \frac{\alpha_{\text{ir}}}{\alpha} \left(\frac{\partial \ln \alpha_{\text{ir}}}{\partial \ln V} \right)_T$	$\left(\frac{\partial \ln \alpha}{\partial T} \right)_V = \frac{\alpha_{\text{el}}}{\alpha} \left(\frac{\partial \ln \alpha_{\text{el}}}{\partial T} \right)_V + \frac{\alpha_{\text{ir}}}{\alpha} \left(\frac{\partial \ln \alpha_{\text{ir}}}{\partial T} \right)_V$ ($10^{-5}/^\circ\text{K}$)
PbF ₂	0.46	0.54	1.48 = 0.25 + 1.23	-6.00 = -0.67 - 5.33
CaF ₂	0.39	0.61	2.06 = 0.23 + 1.83	3.83 = -0.05 + 3.88
BaF ₂	0.41	0.59	1.88 = 0.14 + 1.74	...

contribute significantly to the measured temperature dependence of ϵ' for the crystals of present interest. This is especially so for cubic PbF_2 .

2. Anharmonic model results

A detailed theoretical treatment of the anharmonic contributions to the dielectric constant of ionic crystals has been given by Szigeti¹⁹ and more recently by Cowley.²³ By expanding the potential energy and dipole moment as power series in the ionic displacements Szigeti showed that ϵ' can be written

$$\epsilon' = \epsilon_\infty + \eta + G, \quad (10)$$

where η is the quasiharmonic contribution and G represents the anharmonic contribution. G is a function of the phonon frequencies, phonon occupation numbers, and normal-mode coordinates. By considering η and G to be unique functions of volume and temperature, respectively, Szigeti showed that for temperatures above the Debye temperature, Θ_D , G is given by

$$G = T \left(\frac{\partial(\epsilon' - \epsilon_\infty)}{\partial T} \right)_V, \quad (11a)$$

$$\approx T \left(\frac{\partial \epsilon'}{\partial T} \right)_V, \quad (11b)$$

$$= \frac{T}{3} [(\epsilon' - 1)(\epsilon' + 2)] \left(\frac{\partial \ln \alpha}{\partial T} \right)_V, \quad (11c)$$

where Eq. (11b) follows from the results in Tables I–IV, and Eq. (11c) follows readily from Eq. (2).⁶ G is then readily evaluated from the results in Table II.

By treating η as a unique function of volume, η acquires a temperature dependence since the volume is a function of temperature via the thermal expansion. This leads to a change in η , $\Delta\eta_T$, over and above its strictly harmonic value. This is a quasiharmonic contribution, and for $T > \Theta_D$ it is given by¹⁹

$$\Delta\eta_T \equiv \eta(V_T) - \eta(V_0), \quad (12a)$$

$$= -T \frac{\beta}{\kappa} \left(\frac{\partial(\epsilon' - \epsilon_\infty)}{\partial P} \right)_T, \quad (12b)$$

$$\approx -T \frac{\beta}{\kappa} \left(\frac{\partial \epsilon'}{\partial P} \right)_T, \quad (12c)$$

where the last approximation follows from the data in Tables I and III.

Table V shows the various contributions to ϵ' according to Eq. (10) for the various crystals at 295°K expressed as fractions of the lattice con-

TABLE V. Values at 295°K of the Debye temperatures (Θ_D), dielectric constants (ϵ' and ϵ_∞), lattice parameters (a), inverse reduced mass (μ), and the $\bar{q}=0$ transverse and longitudinal optic mode frequencies (ω_{TO} and ω_{LO}) for a number of crystals having the cubic fluorite structure. Also given are: (i) the electronic enhancement factor $[\frac{1}{3}(\epsilon_\infty + 2)]^2$ to the lattice contribution to ϵ' ; (ii) the strictly harmonic (η_0), the quasiharmonic (η_T) and anharmonic (G) contributions to the lattice contribution to ϵ' ; (iii) the Szigeti effective charge ratios e^*/e ; and (iv) a test of the Lyddane-Sachs-Teller (LST) relation (last two columns).

Crystal	Θ_D (°K)	ϵ'	ϵ_∞	ϵ'_i	$[\frac{1}{3}(\epsilon_\infty + 2)]^2$	$\left(\frac{\eta_0}{\epsilon' - \epsilon_\infty} \right)$	$\left(\frac{\Delta\eta_T}{\epsilon' - \epsilon_\infty} \right)$	$\left(\frac{\eta_T}{\epsilon' - \epsilon_\infty} \right)$	$\left(\frac{G}{\epsilon' - \epsilon_\infty} \right)$	a (Å)	μ^{-1} (10^{22} g^{-1})	ω_{TO} (cm^{-1})	ω_{LO} (cm^{-1})	e^*/e	$\epsilon'/\epsilon_\infty$	$\left(\frac{\omega_{LO}}{\omega_{TO}} \right)^2$
PbF_2	217	29.30	3.08	26.22	2.87	1.077	0.120	1.197	-0.197	5.940	1.88	106 ^a	338 ^a	0.94	9.51	10.17
												102 ^b	337 ^b	0.91	...	10.90
BaF_2	280	7.34	2.17	5.17	1.93	0.910	0.054	0.964	0.036	6.184	2.02	189 ^a	330 ^a	0.92	3.38	3.05
												188 ^c	344 ^c	3.35
SrF_2	380	6.48	2.07	4.41	1.84	0.910	0.058	0.968	0.032	5.860	2.27	219 ^a	382 ^a	0.88	3.13	3.04
												222 ^c	395 ^c	3.16
CaF_2	500	6.81	2.06	4.75	1.83	0.896	0.064	0.960	0.040	5.450	3.08	266 ^a	474 ^a	0.86	3.31	3.18
												263 ^c	482 ^c	3.36

^a Data from Ref. 28.

^b Data from Ref. 29.

^c Data from Ref. 2.

tribution to ϵ' , i.e., $(\epsilon' - \epsilon_\infty)$. It is seen that 295 °K is greater than Θ_D for PbF_2 and BaF_2 , and for these crystals the approximations leading to Eqs. (11) and (12) for G and $\Delta\eta_T$ should be reasonably valid. For SrF_2 and CaF_2 , on the other hand, $295^\circ\text{K} < \Theta_D$ and the results in Table V should be considered as approximate only.

As can be seen from the results in Table V, for the alkaline-earth fluorides at room temperature the quasiharmonic effects represented by $\Delta\eta_T$ and the higher-order anharmonicities represented by G contribute about (5–6)% and (3–4)%, respectively, to the lattice contribution to ϵ' . Both of these contributions are positive and enhance the strictly harmonic contribution η_0 . Furthermore, the quasiharmonic approximation is quite good for these crystals. This is also found to be the case for other normal ionic crystals such as the alkali halides.¹⁹ On the other hand, for cubic PbF_2 both $\Delta\eta_T$ and G are much larger; specifically, G contributes about 20% to the measured $\epsilon' - \epsilon_\infty$, and it is negative, thus acting to reduce the harmonic contribution. The magnitude of G here is such that it more than negates the positive quasiharmonic shift, and it is responsible for the decrease of ϵ' with increasing T . In this regard the behavior of cubic PbF_2 is qualitatively similar to that of the cubic thallos halides⁶ and other weak soft TO mode crystals.²²

The sign of G , or alternatively $(\partial \ln \alpha / \partial T)_V$, can be understood in terms of the different contributions to G .^{19,23,24} To first order, it is found that G consists of two terms. The first is a negative contribution arising from quartic anharmonicities, and the second is positive (at low frequencies) and arises from cubic anharmonicities. The fact that G is strongly negative for cubic PbF_2 indicates the dominance of the quartic anharmonicities in this crystal. This is the case for crystals with soft TO modes.

It is of interest to recall that for the high-pressure orthorhombic phase of PbF_2 $(\partial \ln \alpha / \partial T)_V$, and hence G , is positive. Earlier work on the alkali¹⁴ and thallos⁶ halides showed that the sign of G is crystal structure sensitive, being positive for those crystals having the NaCl structure and negative for crystals with the CsCl structure. A possible explanation was based on the finding that the cubic anharmonicity (which as seen above leads to a positive G) is structure sensitive and decreases as the number of nearest neighbors decreases.¹⁴ Clearly this explanation is not valid for PbF_2 , and, furthermore, it is orthorhombic and not cubic PbF_2 which has the same sign of G as the cubic alkaline-earth fluorides. Thus, crystal structure is not the dominant factor in determining the sign of G for these materials.

3. Magnitude of the dielectric constant

As seen earlier (cf Table II) ϵ' of the alkaline-earth fluorides falls in the range 6–8 whereas ϵ' for PbF_2 is 4–5 times larger. What is the origin of this large ϵ' for PbF_2 ?

Without being concerned about anharmonic effects for this purpose, it is seen from Eq. (9) that ϵ' is given by the sum of an electronic contribution ϵ_∞ and a lattice contribution η_0 (which may also be designated by ϵ'_l). We also note, as was first emphasized by Szigeti,¹⁹ that the electronic polarizabilities of the ions influence η_0 in two different ways: first, via the effective ionic charge e^* —a short-range effect, and secondly, via the factor $[\frac{1}{3}(\epsilon_\infty + 2)]^2$ which arises from long-range interactions between electronic and ionic displacements.

Table V compares the two contributions to ϵ' for cubic PbF_2 and the alkaline-earth fluorides. For the latter crystals values of ϵ'_l are about 2–3 times ϵ_∞ , a circumstance similar to that for many normal ionic crystals such as the alkali halides. For PbF_2 , on the other hand, ϵ'_l dominates ϵ' by far. Unusually large values of ϵ'_l can arise in two different ways (e^* is always $\leq e$, the electronic charge): (i) a large value of the electronic enhancement factor $[\frac{1}{3}(\epsilon_\infty + 2)]^2$, or (ii) an abnormally small value of the resonance frequency ω_{TO} as in the case of soft-mode materials. Values of $[\frac{1}{3}(\epsilon_\infty + 2)]^2$ and ω_{TO} are listed in Table V. Although $[\frac{1}{3}(\epsilon_\infty + 2)]^2$ is somewhat larger for PbF_2 than for the other crystals, it is clearly the much smaller ω_{TO} that is responsible for the large ϵ'_l , and hence ϵ' , of PbF_2 .

4. Curie-Weiss $\epsilon'(T)$ dependence for cubic PbF_2

The $\epsilon'(T)$ response of cubic PbF_2 in Fig. 1 can be well represented between ~50 and 275 °K by a Curie-Weiss law of the form

$$\epsilon' = C / (T - T_0) \quad (13)$$

with $C = 9.29 \times 10^4$ °K and $T_0 = -2890$ °K. This behavior is generally associated with the temperature dependence of ϵ' of ferroelectrics or incipient ferroelectrics above their Curie points, i.e., in the paraelectric phase, and usually foreshadows a transition to a ferroelectric phase. Of course, in the present case T_0 is large and negative and there is no transition. Nevertheless, we believe that the relatively high ϵ' and its Curie-Weiss behavior in cubic PbF_2 are associated with the existence of a soft long-wavelength TO mode (i.e., a ferroelectric mode) in this crystal. Cubic PbF_2 can then be classified as an incipient displacive ferroelectric as are the cubic thallos halides^{16,25} and TiO_2 .²² In fact there is a striking resemblance between the $\epsilon'(T)$ response of these latter crystals

and PbF_2 .

Thus, on the basis of the present work, it is predicted that the ir resonance frequency ω_{TO} of cubic PbF_2 should increase with increasing temperature, unlike the behavior of normal dielectrics. This is because in the soft-mode theory $\epsilon'(T)$ is related to $\omega_{\text{TO}}(T)$ by

$$\omega_{\text{TO}}^2 \propto 1/\epsilon' \propto T - T_0. \quad (14)$$

Unfortunately, the T dependence of ω_{TO} for cubic PbF_2 apparently has not been measured so that we cannot test this prediction. However, we can estimate the magnitude of the effect from the $\epsilon'(T)$ data since from Eq. (14) it follows that

$$2 \left(\frac{\partial \ln \omega_{\text{TO}}}{\partial T} \right)_P \simeq - \left(\frac{\partial \ln \epsilon'}{\partial T} \right)_P. \quad (15)$$

At 295 °K $(\partial \ln \epsilon' / \partial T)_P = -2.4 \times 10^{-4}$ per °K, so that $(\partial \ln \omega_{\text{TO}} / \partial T)_P \simeq +1.2 \times 10^{-4}$ per °K. This is a small change, but it is within the resolution of careful ir and neutron spectroscopy measurements, and it is of the same magnitude as the $(\partial \ln \omega_{\text{TO}} / \partial T)_P \simeq 1.4 \times 10^{-4}$ per °K observed for TlBr at 295 °K.²⁵ For comparison purposes, ω_{TO} decreases with increasing T for the alkaline-earth fluorides, e.g., $(\partial \ln \omega_{\text{TO}} / \partial T)_P \simeq -1.3 \times 10^{-4}$ per °K for BaF_2 at 295 °K.²

The pressure results also support the conclusion that there is a soft ($\vec{q}=0$) TO mode in cubic PbF_2 . As can be seen from Table I, the magnitude of the pressure derivative $\partial \ln \epsilon' / \partial P$ increases with decreasing T for PbF_2 , unlike the behavior of BaF_2 which is typical of normal ionic crystals. The behavior of PbF_2 is typical of crystals with soft TO modes and can be readily understood in terms of soft-mode theory, as has been discussed elsewhere.²²

5. Effective ionic charge e^*

In an ideal crystal consisting of deformable ions which do not overlap, the individual ions can be expected to carry their formal charges $Z_i e$. In real crystals, however, ions overlap, and the concept of an effective charge e^* was first introduced by Szigeti¹⁹ to account for the polarization effects associated with this overlap. The concept arises in a natural way in lattice-dynamical models such as the shell model.²⁶ It should be noted that various forms of the expression for e^* are in use.²⁷ For the present purposes we shall as is most generally the case calculate the so-called Szigeti effective charge defined by Eq. (9). We emphasize that this is a "transverse" effective charge in that it relates to a transverse TO mode.

In the absence of anharmonicities e^* can be calculated directly from Eq. (9) since all other quantities in this equation are either known or measurable. For the alkaline-earth fluorides ϵ' , ϵ_∞ , ν , and ω_{TO} are known at 4 °K, and values of e^*/e have been reported (see, e.g., Ref. 2). For these crystals, Eq. (9) is also a good approximation at room temperature, since, as we have seen earlier, the anharmonic effects are relatively small. In practice there is another justification for using Eq. (9) at high temperature provided that the *measured values* of the various quantities at the appropriate temperature are used. This is because the quasiharmonic and anharmonic contributions to ϵ' are reflected to a large degree in changes in ν and ω_{TO} . This is especially the case in soft-mode crystals such as cubic PbF_2 .²² Here, as we have seen, $\epsilon' \sim 1/\omega_{\text{TO}}^2$ and anharmonic contributions to ϵ' should be reflected faithfully in ω_{TO} , and e^* can then be calculated reasonably accurately from Eq. (9).

Table V summarizes the various appropriate quantities and the calculated values of e^*/e at 295 °K for the crystals of interest. These values were calculated from Eq. (9) using the *measured values* of all the parameters at 295 °K. For the alkaline-earth fluorides the values of e^*/e at 4 °K reported by Lowndes² are systematically slightly lower than our 295 °K values. However, the uncertainties in the measured values of ϵ' , ϵ_∞ , and ω_{TO} make the differences in the e^*/e values at the two temperatures well within experimental uncertainty. For PbF_2 our value of e^*/e at 295 °K is 0.94. This is based on the Denham *et al.*²⁸ value of 106 cm^{-1} for ω_{TO} . If instead we use the earlier value of Axe *et al.*²⁹ 102 cm^{-1} , we obtain $e^*/e = 0.91$. Earlier, Axe *et al.*,²⁹ using calculated values of ϵ' and ϵ_∞ and the measured $\omega_{\text{TO}} = 102 \text{ cm}^{-1}$, reported $e^*/e = 0.87$.

It is interesting to note that the above values of e^*/e are of the same magnitude as those for the alkali halides.^{16,30} The theoretical interpretation of the deviation of e^*/e from unity in terms of the various contributions to this deviation has been attempted for the alkali halides by several authors.^{26,30,31} The results show that less than one-half of the deviation results from electronic distortions associated with the overlap of adjacent ions and that the remainder is associated with Coulomb (long-range) interactions which can induce multipole distortion of the ions. The situation is most likely qualitatively similar for the present fluorite crystals, but apparently no specific theoretical treatments have been attempted. Such treatments have to be based on a detailed knowledge of the electronic structure of the various ions.

6. Lyddane-Sachs-Teller relation

An important and useful relationship for ionic crystals is the Lyddane-Sachs-Teller (LST) relation. It relates the dielectric constants ϵ' and ϵ_∞ to the zone-center longitudinal (LO) and transverse (TO) optic phonons. In the absence of damping, the LST relation for a cubic crystal with one TO and one LO mode (which is the case for the present crystals) is

$$\epsilon'/\epsilon_\infty = (\omega_{\text{LO}}/\omega_{\text{TO}})^2. \quad (16)$$

This equation is derived in the harmonic approximation, but in practice it is found to hold well for crystals with considerable anharmonicities, e.g., soft-mode ferroelectrics. This is because the measured ϵ' 's and the frequencies are effectively renormalized by the anharmonicities and represent the true response of the crystal.

Table V compares measured values of $\epsilon'/\epsilon_\infty$ at 295 °K with values calculated from the measured frequencies via Eq. (16). It is seen that for the four crystals Eq. (16) is generally valid to about 10%. Unfortunately there are substantial differences in the frequencies reported by the different authors, and these also lead to variations up to ~10% in the calculated $\epsilon'/\epsilon_\infty$ for each crystal. Nevertheless, some qualitative remarks can be made about the results in Table V. The calculated ratio $(\omega_{\text{LO}}/\omega_{\text{TO}})^2$ appears to be less than or equal to the measured ratio $\epsilon'/\epsilon_\infty$ for the alkaline-earth fluorides, but the opposite is true for PbF_2 . This observation stands out if we emphasize the Denham *et al.*²⁸ values of the frequencies. These authors reported ω_{LO} and ω_{TO} for all four crystals, and this should minimize systematic differences in these quantities.

A likely explanation for the large calculated ratio $(\omega_{\text{LO}}/\omega_{\text{TO}})^2$ for PbF_2 is the presence of relatively large damping in this crystal.^{28,29} In the presence of damping the LST relation involves the magnitudes of the complex frequencies rather than the real parts,^{29,32} and this tends to reduce the calculated ratio and bring it closer to the measured ratio $\epsilon'/\epsilon_\infty$.

C. Phase transition

It has long been recognized that, in addition to the eight-coordinated cubic fluorite phase ($Fm\bar{3}m-O_h^5$), PbF_2 can also exist at normal conditions in the orthorhombic α - PbCl_2 -type structure ($Pmnb-V_{2h}^{16}$) which is a quasi-nine-coordinated structure—each Pb ion has nine near, but not equidistant, F neighbors. In both phases there are four molecules per unit cell, but there is an ~10% increase in density¹¹ on going to the orthorhombic

phase. The orthorhombic phase should then be the favored form at high pressure, and a pressure-induced transition from cubic to orthorhombic can be expected. Such a transition does indeed occur, as we have seen earlier. The transition was first observed by Schmidt and Vedam¹¹ who reported a transition pressure of 4.8 kbar at 295 °K. Kesler *et al.*³³ reported the Raman spectrum of the high-pressure phase and confirmed that the structure is indeed orthorhombic α - PbCl_2 -type.

Similar pressure-induced transitions occur in the alkaline-earth fluorides.³⁴ Of these, the best characterized transition is that in BaF_2 which occurs at ~27 kbar at 295 °K.⁴ It has been suggested⁴ that this transition may in part be associated with the softening of the [110] transverse acoustic (TA) phonon branch. More recently, shell-model calculations³⁵ of the dispersion relations of cubic PbF_2 showed that the TA mode frequencies along the major directions were imaginary at large wave vectors. These results of course simply indicate that the model and parameters used did not lead to a stable lattice. However, we know that cubic PbF_2 is metastable or just barely stable at normal conditions. This suggests that the calculations may not be far wrong, and, in any case, the calculations along with the experimental results suggest the desirability of examining the pressure dependence of the phonon dispersion curves of PbF_2 .

As expected, the properties of the transition in PbF_2 and BaF_2 are very similar. In BaF_2 the cubic and orthorhombic phases coexist over a wide pressure range (see Fig. 3), and PbF_2 has the additional feature that the orthorhombic phase is recovered after releasing the pressure. Figure 11 shows that the cubic-orthorhombic transition pressure, P_t , for PbF_2 decreases with increasing T , but the transition cannot be induced by increasing T alone at 1 bar. Because of the irreversibility of the transition each datum point in Fig. 11 is from a separate sample. The results in Fig. 11 are qualitatively similar to those reported earlier⁴ for BaF_2 , and it can be anticipated that the more complete P - T phase diagram for PbF_2 is also qualitatively similar to that proposed for BaF_2 .⁴

Assuming the measured dP_t/dT for the transition is close to the equilibrium value, it follows that the Clapeyron equation $dP_t/dT = \Delta S/\Delta V$ holds. Here ΔS and ΔV are the discontinuous changes in entropy and volume at P_t . For PbF_2 at 295 °K we estimate $\Delta V \approx -0.0126 \text{ cm}^3/\text{g}$ from Schmidt and Vedam's¹¹ lattice parameter data (assuming that the compressibilities of the two phases are the same) and from Fig. 11 $dP_t/dT \approx -36 \text{ bar}/^\circ\text{K}$. Using these values in the above equation yields $\Delta S \approx 2.6 \text{ cal/g mole }^\circ\text{K}$. The corresponding quantities for BaF_2 are quite com-

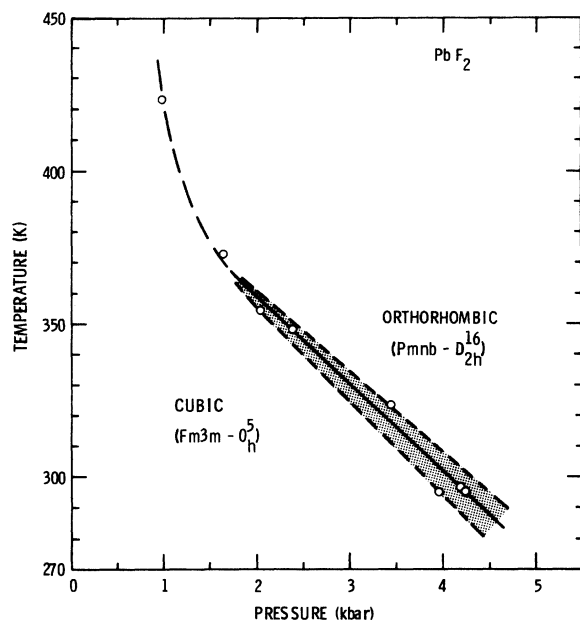


FIG. 11. Temperature dependence of the cubic-to-orthorhombic transition pressure for PbF_2 . Shaded region denotes the range of transition pressures observed.

parable and are⁴: $\Delta V = -0.022 \text{ cm}^3/\text{g}$, $dP_t/dT \approx -26 \text{ bar}/^\circ\text{K}$, and $\Delta S \approx 2.4 \text{ cal/g mole } ^\circ\text{K}$.

Although the dielectric constant ϵ' increases by 40% in PbF_2 and by 34% in BaF_2 at the cubic \rightarrow orthorhombic transition, examination of these changes in conjunction with Eq. (2) and the known volume changes at the transition reveals that the total polarizability α decreases by 5.5% in PbF_2 and 1.5% in BaF_2 on going to the orthorhombic phase. These findings can be qualitatively understood on the basis that the polarizability of a group of ions can be expected to decrease as the volume available for ionic displacements decreases, and, furthermore, for a given decrease in volume, the decrease in α can be expected to be larger the larger the initial α .

D. Frequency-dependent effects in PbF_2

In addition to electronic and ir polarization, another important possible contribution to the static dielectric properties of a substance is dipolar polarization associated with either permanent dipoles (not present in the crystals of interest here) or dipoles produced by impurities and lattice defects. These contributions are not completely independent; however, they exhibit different frequency responses. At very low frequencies all three processes contribute, whereas at optical frequencies only the electronic polarization contributes. Since in the present work we are dealing with measuring frequencies orders of magnitude

below the ir resonance frequency, the strong frequency and temperature dependences of ϵ' and ϵ'' of PbF_2 observed at the higher temperatures in Figs. 1, 4, 7, and 8 can be attributed to dipolar effects. These effects are not seen in the alkaline-earth fluorides over the range of temperatures (up to 350 $^\circ\text{K}$) covered in the present work, but can be expected at higher temperatures. The reason why these dipolar effects are quite large for PbF_2 (both phases) at 300 $^\circ\text{K}$ can be attributed to the fact that this crystal is already a good ionic conductor at this temperature, with conductivity ($\sim 10^{-6} \Omega^{-1} \text{ cm}^{-1}$) orders of magnitude larger than for the other crystals.

The dipolar effects of interest here are controlled by the formation and motion of defects, and these are activated processes. At sufficiently high temperature the dielectric loss becomes dominated by the conductivity σ of the sample and is given by⁶

$$\tan \delta = \epsilon''/\epsilon' = 4\pi\sigma/\epsilon'\omega, \quad (17)$$

where ω is the measuring frequency, and σ can be written

$$\sigma = \sigma_0 e^{-E/kT}, \quad (18)$$

where E is the activation energy.

Figure 12 shows ϵ'' vs $1/T$ for cubic PbF_2 . It

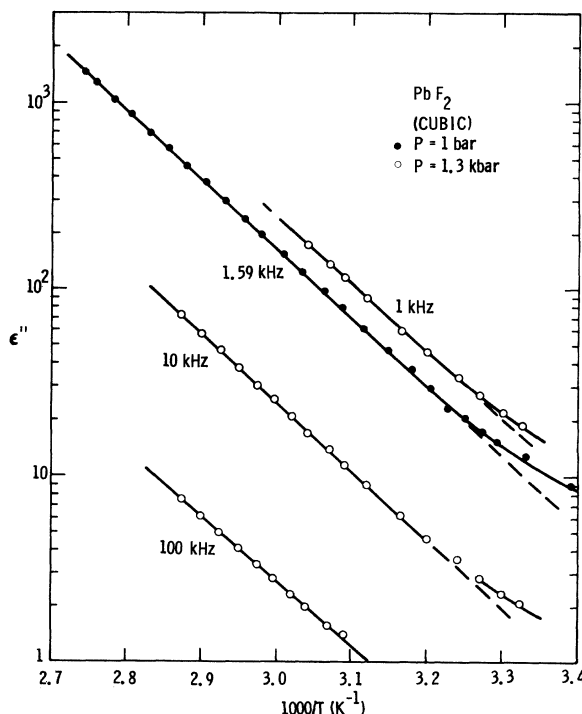


FIG. 12. Imaginary part of the dielectric constant of cubic PbF_2 as a function of inverse temperature. ϵ'' is directly related to the conductivity of the sample, and the slopes yield the activation energies.

is seen that the data exhibit the frequency and temperature dependence expected from Eqs. (17) and (18). Above $\sim 310^\circ\text{K}$ the response is linear with $E = 0.72$ eV at 1 bar. This is in excellent agreement with the activation energy determined from ionic conductivity measurements in the same temperature regime.^{36,37} A more detailed investigation of the effects of pressure on the ionic conductivity of both phases of PbF_2 , including the behavior at the transition, will be presented elsewhere.³⁷

V. SUMMARY AND CONCLUSIONS

The main results and conclusions of the present work can be summarized as follows.

(a) Analysis of the temperature and pressure dependences of the static dielectric constants, ϵ' , of the alkaline-earth fluorides and PbF_2 shows that the quasiharmonic approximation is quite good for the alkaline-earth fluorides but that anharmonicities (quartic) dominate $\epsilon'(T)$ of cubic PbF_2 .

(b) These anharmonicities cause ϵ' of cubic PbF_2 to increase with decreasing T and obey a Curie-Weiss law over a substantial temperature range. We attribute this behavior and the relatively large ϵ' of this crystal to the existence of a soft ferroelectric mode.

(c) For the orthorhombic phase of PbF_2 , ϵ' decreases with decreasing T as is true of normal ionic crystals.

(d) Although ϵ' increases by 40% in PbF_2 and

by 34% in BaF_2 at the pressure-induced cubic \rightarrow orthorhombic transition, it is found that the total polarizability α decreases by 5.5% in PbF_2 and 1.5% in BaF_2 on going to the orthorhombic phase. These findings can be understood on the basis of simple qualitative arguments.

(e) The effect of temperature on the transition pressure of PbF_2 was investigated and the thermodynamic properties of the transition determined.

(f) Values of the Szigeti effective charge ratio e^*/e for the crystals of present interest are found to be the range 0.86–0.94. Causes for this deviation from unity are briefly discussed.

(g) The LST relationship holds to within 10% for the crystals of interest. The main uncertainty is in the values of the TO and LO phonon frequencies.

(h) The dielectric properties of PbF_2 exhibit strong frequency and T dependences at $T \geq 300^\circ\text{K}$. These effects are attributed to lattice defects and the relatively high ionic conductivity of this crystal in both phases.

ACKNOWLEDGMENTS

It is a pleasure to acknowledge the expert technical assistance of B. E. Hammons in carrying out the experiments. Thanks are also due to B. Morosin for making his thermal expansion data on cubic PbF_2 available prior to publication and to P. S. Peercy for helpful discussions.

*Work supported by the Energy Research and Development Administration.

¹B. W. Jones, *Philos. Mag.* **16**, 1085 (1967).

²R. P. Lowndes, *J. Phys. C* **2**, 1595 (1969); **4**, 3083 (1971).

³C. Andeen, D. Schuele, and J. Fontanella, *Phys. Rev. B* **6**, 591 (1972).

⁴G. A. Samara, *Phys. Rev. B* **2**, 4198 (1970).

⁵G. A. Samara, *J. Phys. Chem. Solids* **26**, 121 (1965).

⁶G. A. Samara, *Phys. Rev.* **165**, 959 (1968).

⁷D. Gerlich, *Phys. Rev.* **135**, A1331 (1964); **136**, A1366 (1964); *Phys. Rev. B* **1**, 2718 (1970).

⁸C. Wong and D. E. Schuele, *J. Phys. Chem. Solids* **29**, 1309 (1968).

⁹P. W. Bridgman, *Proc. Am. Acad. Arts Sci.* **77**, 189 (1949).

¹⁰S. Hart, *J. Phys. D* **3**, 430 (1970). The earlier values of the c_{ij} of J. H. Vasilik and M. L. Wheat [*J. Appl. Phys.* **36**, 791 (1965)] are in error owing to sample misorientation.

¹¹E. D. D. Schmidt and K. Vedam, *J. Phys. Chem. Solids* **27**, 1563 (1966).

¹²A. C. Bailey and B. Yates, *Proc. Phys. Soc. Lond.* **91**, 390 (1967).

¹³B. Morosin (private communication).

¹⁴A. J. Bosman and E. E. Havinga, *Phys. Rev.* **129**, 1593 (1963); **140**, A292 (1965).

¹⁵H. Fröhlich, *Theory of Dielectrics* (Clarendon, Oxford, England, 1949), Appendix 3, p. 169.

¹⁶G. A. Samara, in *Materials Under Pressure*, Honda Memorial Series, edited by T. Hirone (Maruzen Company, Ltd., Tokyo, 1974), Vol. 2, p. 179.

¹⁷R. S. Krishnan, *Progress in Crystal Physics*, (S. Viswanathan, Madras, 1958), Vol. I, p. 26.

¹⁸D. A. Jones, *Proc. Phys. Soc. Lond. B* **68**, 165 (1955).

¹⁹B. Szigeti, *Trans. Faraday Soc.* **45**, 155 (1949); *Proc. R. Soc. Lond. A* **204**, 51 (1950); **A 252**, 217 (1959); **A 261**, 274 (1961).

²⁰J. D. Axe, *Phys. Rev.* **139**, A1215 (1965).

²¹The long wavelength ($\vec{q}=0$) displacements of the ions in the unit cell of the cubic fluorite structure ($O_h^5-Fm\bar{3}m$) transform as $2F_{1u} + F_{2g}$. One of the F_{1u} representations corresponds to the three acoustic branches (one LA and a doubly degenerate TA) and the other to the ir-active modes (one LO and a doubly degenerate TO). The F_{2g} representation corresponds to the triply degenerate Raman-active mode. Thus there is only one TO phonon at $\vec{q}=0$.

- ²²See, e.g., G. A. Samara and P. S. Peercy, *Phys. Rev. B* 7, 1131 (1973); see also Ref. 2.
- ²³R. A. Cowley, *Adv. Phys.* 12, 421 (1963); *Philos. Mag.* 11, 673 (1965).
- ²⁴R. Fuchs, Technical Report No. 167, Laboratory for Insulation Research, MIT, Cambridge, Mass., 1961 (unpublished).
- ²⁵R. P. Lowndes, *Phys. Rev. Lett.* 27, 1134 (1971).
- ²⁶See, e.g., A. G. Dick and A. W. Overhauser, *Phys. Rev.* 112, 90 (1958).
- ²⁷See, e.g., J. C. Phillips, *Rev. Mod. Phys.* 42, 317 (1970); G. Lucovsky, R. Martin, and E. Burstein, *Phys. Rev. B* 4, 1367 (1971); P. Lawaetz, *Phys. Rev. Lett.* 26, 697 (1971).
- ²⁸P. Denham, G. R. Field, P. L. R. Morse, and G. R. Wilkinson, *Proc. R. Soc. Lond. A* 317, 55 (1970).
- ²⁹J. D. Axe, J. W. Gaglianella, and J. E. Scardefield, *Phys. Rev.* 139, A1211 (1965).
- ³⁰R. P. Lowndes and D. H. Martin, *Proc. R. Soc. Lond. A* 308, 473 (1969).
- ³¹V. V. Mitskevich, *Fiz. Tverd. Tela* 5, 3500 (1963) [*Sov. Phys.-Solid State* 5, 2568 (1964)].
- ³²A. S. Barker, Jr., *Phys. Rev.* 136, A1290 (1964).
- ³³J. R. Kessler, E. Monberg, and M. Nicol, *J. Chem. Phys.* 60, 5057 (1974).
- ³⁴D. P. Dandekar and J. C. Jamieson, *Trans. Am. Crystallogr. Assoc.* 5, 19 (1969).
- ³⁵V. Ramachandran and R. Srinivassan, *Solid State Commun.* 11, 973 (1972).
- ³⁶C. E. Derrington and M. O'Keeffe, *Nat. Phys. Sci.* 246, 44 (1973).
- ³⁷G. A. Samara (unpublished).

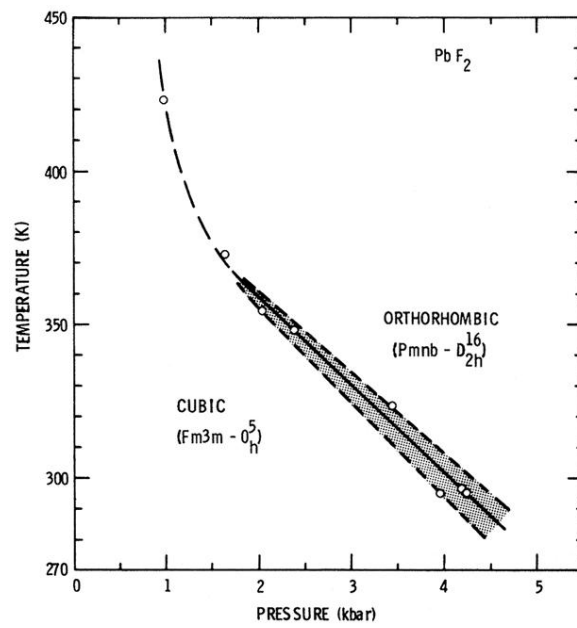


FIG. 11. Temperature dependence of the cubic-to-orthorhombic transition pressure for PbF_2 . Shaded region denotes the range of transition pressures observed.